

## ADVANCED RECHARGEABLE SODIUM BATTERIES WITH NOVEL CATHODES

S. Di Stefano, B.V. Ratnakumar and C.P. Bankston  
Jet Propulsion Laboratory  
California Institute of Technology  
Pasadena, California 91109

Abstract

Various high energy density rechargeable batteries are being considered for future space applications. Of these, the sodium sulfur battery is one of the leading candidates. The primary advantage is the high energy density (760 Wh/kg theoretical). Energy densities in excess of 180 Wh/kg have been realized in practical batteries. More recently, cathodes other than sulfur are being evaluated. We at JPL are evaluating various new cathode materials for use in high energy density sodium batteries for advanced space applications. Our approach is to carry out basic electrochemical studies of these materials in a sodium cell configuration in order to understand their fundamental behaviors. Thus far our studies have focused on alternate metal chlorides such as  $\text{CuCl}_2$  and organic cathode materials such as TCNE.

Introduction

Rechargeable batteries play a significant role in NASA's space programs including planetary missions and satellite applications such as Geosynchronous Earth Orbit (GEO) and Low Earth Orbit (LEO) missions. There is an increasing need for a light weight high energy battery with long active and cycle lives. Typically, the efforts at various organizations are aimed at developing a battery system with an energy density  $\geq 200$  Wh/kg at power densities  $\geq 100$  W/kg, cycle life of 1000 cycles and active life of ten years. The interest for many years has been focussed on sodium-sulfur battery which has a high formula energy density (~750 wh/kg) a good portion of which has been realized in practical cells for several hundreds of charge/discharge cycles (1). The battery typically operates at 300-400°C where the  $\beta$ " alumina solid electrolyte (BASE) is highly conductive to sodium ions allowing high power densities drawn from the battery. Together with these advantages, there are certain deterrent factors associated with the use of the sodium sulfur battery which partly protracted the development. R. M. Dell et al. (2) have given an excellent account of the status of the NaS battery in their recent review. Many of these operational and safety problems stem from sulfur electrode, e.g., the excessively corrosive nature of the discharge product, sodium polysulfide, towards steels, the high vapor pressure of liquid sulfur above 700°C, the possible degradation of BASE in polysulfide melts, (3) the insulating nature of liquid sulfur, in particular the way in which it

isolates regions of BASE during recharge, etc. Alternatives to liquid sulfur cathode are therefore being sought and there are some examples in the literature based on fused salt electrolytes (4-6). In this paper, we review our studies on alternate organic and inorganic cathodes in sodium batteries. In both cases, the cell contains sodium tetrachloroaluminate as the secondary molten electrolyte and BASE as primary electrolyte.

Carbonitriles are a class of relatively stable organic compounds that have high reduction potentials and energy densities. Tetracyanoethylene (TCNE) in particular has an energy density of  $\sim 620$  Wh/kg at a high potential of  $\sim 3.0$  V vs.  $\text{Na}^+/\text{Na}$  and a low melting point. Therefore, TCNE has been examined as a possible liquid cathode in sodium batteries. Among the inorganic cathode materials, transition metal dichlorides (e.g.,  $\text{FeCl}_2$  and  $\text{NiCl}_2$ ) are gaining increasing attention as solid, insoluble rechargeable cathodes in place of liquid sulfur (8-11). These systems can operate at lower temperatures  $\sim 170^\circ\text{C}$ , where the corrosion problems are proportionately less severe. The safety problem is considerably reduced due to the inherent sluggish kinetics of the chemical reaction between liquid sodium and  $\text{NaAlCl}_4$  molten electrolyte in the event of ceramic failure (12). Further, the molten electrolyte remains invariant during charge/discharge preventing polarization losses and localized high current densities on the BASE surface. High energy densities  $\sim 150$  Wh/kg and long cycle life have been demonstrated with ferrous chloride and more recently with nickel chlorides. We summarize below our electrochemical studies on the ferrous chloride and nickel chloride cathodes and also on another promising metal chloride, copper chloride.

### Experimental

The experimental cell adopted for these studies is described in detail in (7). The cell essentially has a central-cathode design with a provision to seal the anode half-cell. The cell is heated electrically with a heating tape wound around a stainless steel tube acting as a container for sodium. For the studies involving TCNE, either Pt or C is used as the positive current collector. Metal chloride positive electrodes were initially fabricated by impregnating commercially available sintered nickel grids (used in Ni-Cd batteries) with the depolarizer by immersing the grid into a concentrated chloride solution. Copper electrodes cannot however be made in this manner for long-term studies due to the preferential dissolution of nickel to copper in the impregnating solution. Perforated copper grids were therefore used to make electrodes in the discharged state either by hot pressing with a binder (Teflon) or by sintering the powders in an inert atmosphere at temperatures below the melting point of NaCl. Conventional electrochemical equipment consisting of E G & G 273 potentiostat/Galvanostat and E G & G 5301 lock-in amplifier interfaced with an Apple IIe computer were used. AC and dc measurements were carried out using E G & G ac impedance and Softcorr software. Various techniques such as potentiodynamic polarization, dc linear polarization and ac impedance were employed to obtain information on the kinetic parameters of the cathode

reactions. Discharge/charge cycling was also carried out galvanostatically in a controlled fashion using the above electrochemical equipment. All the chemicals TCNE,  $\text{NaAlCl}_4$ ,  $\text{NaCl}$  and metal powder were of analytical grade and were used as received. BASE tubes were cleaned by etching in hot phosphoric acid. All the cell fabrication operations were carried out in an argon-filled glove box.

## Results and Discussions

The findings of our studies on TCNE as a cathode material in sodium batteries are described in detail elsewhere. (7) Briefly, TCNE reduces at 3.0 V vs.  $\text{Na}^+/\text{Na}$  reversibly with a coulombic yield of >60% at  $1 \text{ mA/cm}^2$  on either the Pt or C current collector. Fig. 1 gives the typical voltage-time curves of TCNE during discharge and charging. The exchange current density on either Pt or C is of the order of  $10^{-3} \text{ A/cm}^2$  in a catholyte containing typically 10% of TCNE. The kinetics of TCNE reduction are essentially governed by the rate of mass transfer in the cathode as evidenced from ac impedance and dc potentiodynamic polarization data. In TCNE-rich catholytes there is a kinetic hindrance to the reduction of TCNE reflected in increased polarization (ohmic, concentration as well as charge transfer) losses. As a result, the coulombic yield as well as diffusion coefficient of TCNE decrease with increasing TCNE concentration in the catholyte. The sluggish kinetics at higher TCNE concentrations is related to the degradation processes occurring in TCNE at operating temperatures of  $\sim 230^\circ\text{C}$  forming an adduct. FTIR studies point to a possible polymerization of TCNE under the experimental conditions. Due to the sluggish kinetics at higher TCNE concentrations, it may not be possible to achieve high power densities from TCNE. On the other hand, for medium to low power applications, TCNE is a good cathode material, since the electrochemical activity and reversibility of TCNE are retained even after polymerization.

### Metal Dichloride Cathodes

Figure 2 shows the typical charge/discharge curves of a  $\sim 16 \text{ mAh}$   $\text{NiCl}_2$  electrode (made by impregnating  $\text{NiCl}_2$  into sintered Ni plaque) at  $200^\circ\text{C}$  and at  $2 \text{ mA/cm}^2$  in the first two test cycles. The discharge as well as charging curves are flat at nominal voltages of 2.56 and 2.63 V vs.  $\text{Na}^+/\text{Na}$  respectively. There is not much polarization loss from the open circuit voltage of 2.59 V.

The coulombic yield is nearly 100% and there is no loss in capacity during cycling in the first few test cycles. Figure 3 illustrates the high rate discharge capability of the electrode. The discharge curves at higher current densities, i.e.,  $4 \text{ mA/cm}^2$  and  $8 \text{ mA/cm}^2$  are also flat with mid-point voltages of 2.54 and 2.5 V and coulombic yields of 98% and 90% respectively. Ferrous chloride electrodes (made by sintering dry powders of sodium chloride and iron) exhibit a lower operating potential of  $\sim 2.3 \text{ V}$  as may be seen from the discharge and charge curves of a  $\sim 230 \text{ mAh}$  electrode in Figure 4. The discharge curve is flat in this case also, with a

coulombic yield in excess of 90%. The copper chloride cathode is expected to give higher voltage than nickel chloride, from the electrode potentials of  $\text{Cu}^{+2}/\text{Cu}$  and  $\text{Ni}^{2+}/\text{Ni}$  couples. Accordingly, higher energy densities may be possible with copper chloride as compared to ferrous chloride or nickel chloride especially at high power densities due to a high electronic conductivity of copper formed in the course of discharge. The essential requirement for a successful operation of metal chloride cathode in the above sodium batteries is total insolubility of the chloride in a  $\text{NaAlCl}_4$  melt. Analytical studies carried out on the catholyte with  $\text{CuCl}_2$  and  $\text{NiCl}_2$  revealed no extra dissolution of copper over nickel. Initial studies with copper chloride (electrode made by impregnation of  $\text{CuCl}_2$  into sintered Ni plaque) show a higher operating voltage than  $\text{NiCl}_2$  or  $\text{FeCl}_2$  (Figure 5). The discharge (as well as charging) curve is, however, not flat in this case as with  $\text{FeCl}_2$  or  $\text{NiCl}_2$  which may be due to the mechanism of reduction being different with the possible formation of a monovalent copper.

DC polarization studies were carried out on these cathode materials to obtain information on the kinetics of their reduction. The potentiodynamic polarization curves of  $\text{NiCl}_2$ ,  $\text{FeCl}_2$  and  $\text{CuCl}_2$  (Figure 6) illustrate the high rate capability of these electrodes. There exist mass transfer effects at high discharge rates interfering with the charge transfer processes due to which limiting currents are observed at high overpotentials  $\geq 300$  mV. The limiting currents may be due to a relatively slow diffusion processes inside the porous cathode. Nevertheless, the limiting current densities are reasonably high and are of the order of 15-25  $\text{mA}/\text{cm}^2$ . The charge transfer kinetics appear to be rapid as evidenced by high exchange current densities of 2  $\text{mA}/\text{cm}^2$ , 0.65  $\text{mA}/\text{cm}^2$  and 0.4  $\text{mA}/\text{cm}^2$  for  $\text{NiCl}_2$ ,  $\text{FeCl}_2$  and  $\text{CuCl}_2$ , respectively, based on the geometric areas of these electrodes. Linear polarization experiments (i.e., at low perturbations) were also carried out to derive similar information on the exchange current densities. The current potential curves at these potentials are linear (e.g.,  $\text{FeCl}_2$  in Figure 7) the slopes of which give the polarization resistances. The exchange current densities thus obtained are 4.6  $\text{mA}/\text{cm}^2$ , 1.5  $\text{mA}/\text{cm}^2$  and 0.39  $\text{mA}/\text{cm}^2$  for  $\text{NiCl}_2$ ,  $\text{FeCl}_2$  and  $\text{CuCl}_2$ , respectively.

The complex plane impedance spectrum of  $\text{NiCl}_2$  (Figure 8) shows a large inductance at high frequencies not shown in the figure attributed to the porous nickel grid and a low frequency semi-circle ascribed to charge transfer kinetics. The exchange current density calculated therefrom is 6.9  $\text{mA}/\text{cm}^2$ . There is no evidence of diffusional impedance in the frequency range studied (i.e.,  $\geq 0.01$  Hz). The complex plane impedance spectrum of  $\text{CuCl}_2$  (sintered) electrode, on the other hand, contains two relaxation loops. The exchange current density evaluated from the first relaxation loop is 0.9  $\text{mA}/\text{cm}^2$ . It is however not clear yet as to whether the second relaxation loop is related to the formation, if any, of monovalent copper during the reduction of  $\text{CuCl}_2$ .

## Conclusions

Among the cathode materials studied at JPL as alternatives to sulfur cathode in sodium batteries, TCNE is suitable for low to medium power applications. Metal dichloride cathodes, on the other hand can deliver energy densities comparable to sodium-sulfur batteries at high power densities without many of the operational and safety problems associated with the use of sodium-sulfur batteries and are thus suitable for various applications including space, EV load-levelling, etc. The electrochemical studies carried out so far indicate high exchange current densities for the reduction of these cathodes.

## Acknowledgement

The work described here was carried out at the Jet Propulsion Laboratory, California Institute of Technology, under contract with the National Aeronautics and Space Administration. One of the authors (B. V. Ratnakumar) acknowledges the National Research Council for providing his Research Associateship during this work.

## References

1. J. Sudworth and A. R. Tilley (Eds.), "The Sodium/Sulfur Battery," Chapman and Hall, New York 1985.
2. R. M. Dell and R. J. Bones, B. Electrochem., 4, 319 (1988).
3. M. Liu and L. C. De Jonghe, J. Electrochem. Soc., 135, 741 (1988).
4. J. Werth, U.S. Patent 3,877,984 (1975).
5. G. Mamantov, R. Marassi, M. Matsunaga, Y. Ogata, J. P. Wiaux and E. J. Frazer, J. Electrochem. Soc., 127, 2319 (1980).
6. K. M. Abraham, L. Pitts and R. Schiff, J. Electrochem. Soc., 127, 2595 (1980).
7. B. V. Ratnakumar, S. Di Stefano, G. Nagasubramanian, R. M. Williams and C. P. Bankston, Extd Abstr. #74, ECS Fall Meeting, Chicago, IL, October 9-14, 1988. Manuscript submitted for publication.
8. J. Coetzer and M. Thackeray, U.S. Patent 4,288,506.
9. J. Coetzer, J. Power Sources, 18, 377 (1986).
10. R. C. Galloway, J. Electrochem. Soc., 134, 286 (1987).
11. B. J. Jones, J. Coetzer, R. C. Galloway and D. A. Teagle, J. Electrochem. Soc., 134, 2379 (1987).
12. R. T. Wedlake, A. R. Tilley and D. A. Teagle, B. Electrochem., 4, 41 (1988).

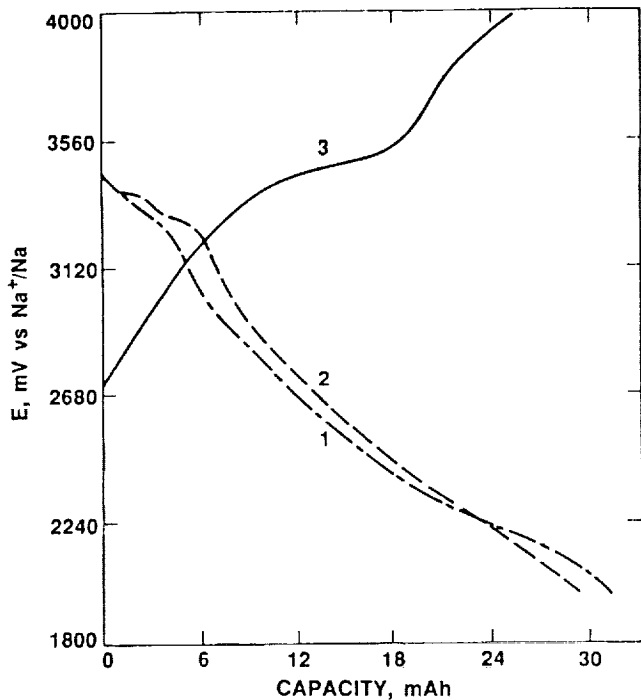


Figure 1. Typical Charge/Discharge Curves of TCNE (10 W<sub>3</sub>) at 230°C: (1) Fourth Discharge, (2) Fifth Discharge, and (3) Charge

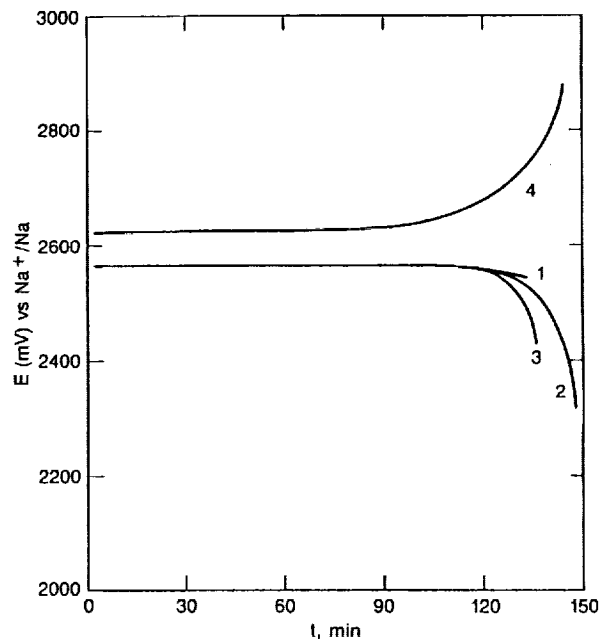


Figure 2. Typical Charge/Discharge Curve 16 mAh Electrode at 200°C During (1) Second, (2) Third, (3) Fourth Discharge, and (4) Charge at 2 mA/cm<sup>2</sup>

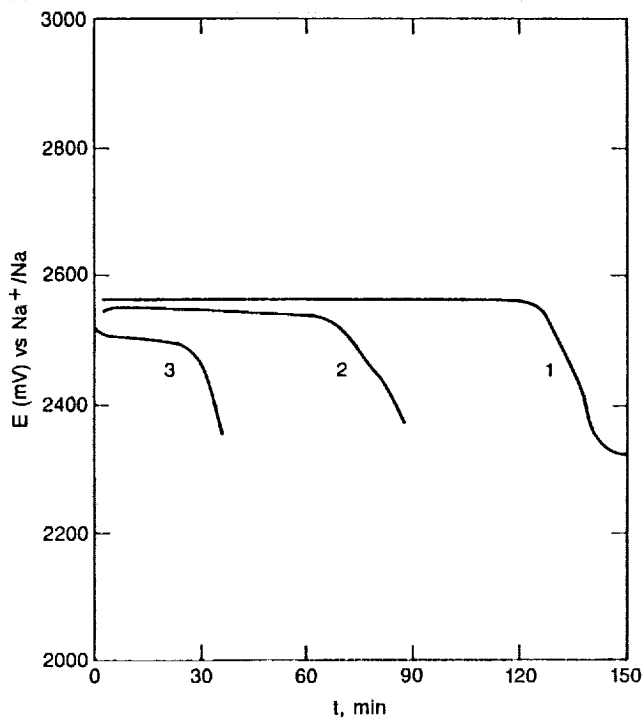


Figure 3. Discharge Curves of 16 mAh NiCl<sub>2</sub> Electrode at 200°C and at Current Density of (1) 2 mA/cm<sup>2</sup>, (2) 4 mA/cm<sup>2</sup>, and (3) 8 mA/cm<sup>2</sup>

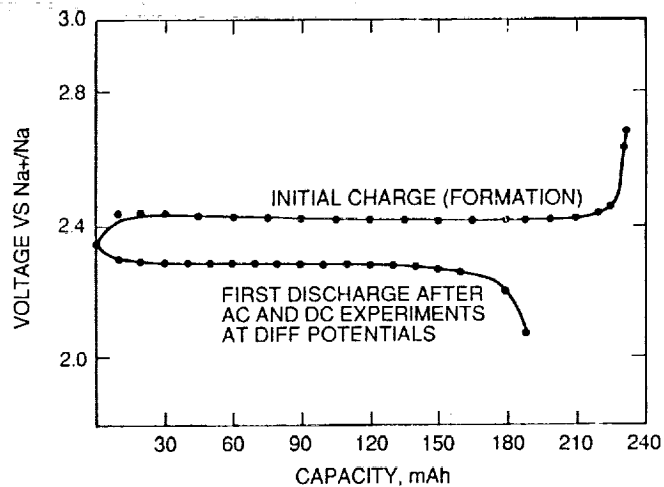


Figure 4. Initial Charge/Discharge Curves of FeCl<sub>2</sub> Cathode

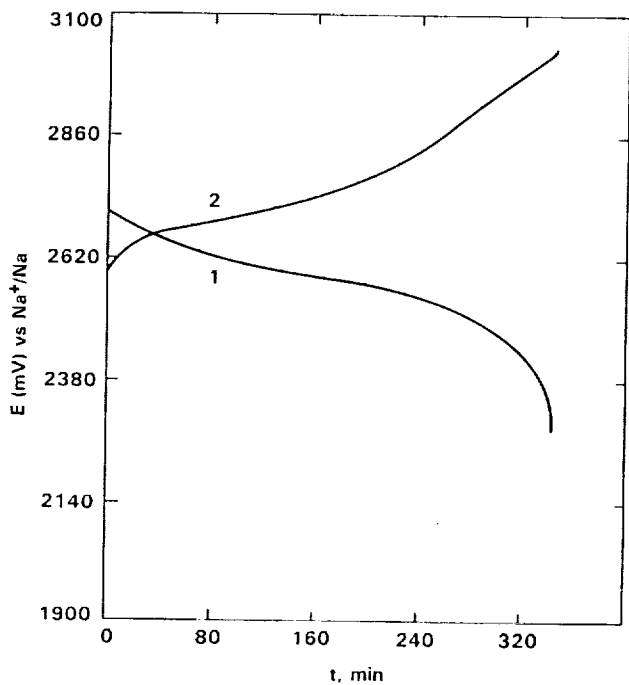


Figure 5. Charge/Discharge Curves of  $\text{CuCl}_2$  Electrode (Made by Impregnating  $\text{CuCl}_2$  into a Sintered Nickel Grid) at  $200^\circ\text{C}$

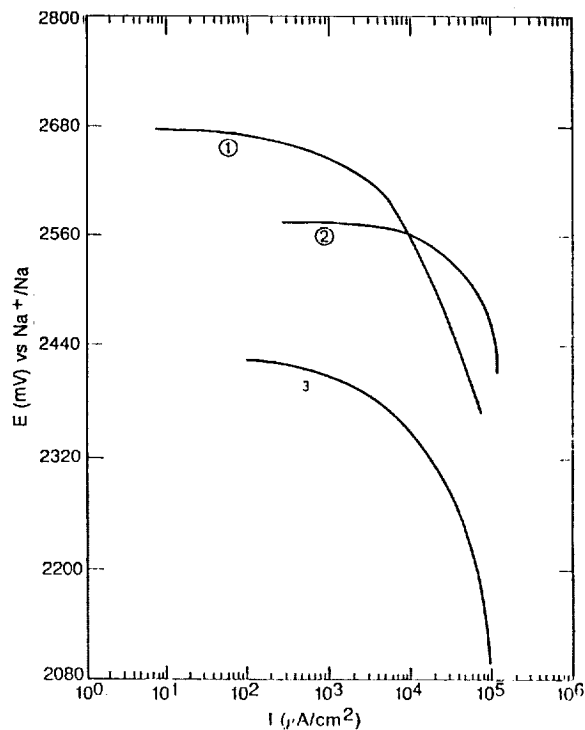


Figure 6. Potentiodynamic Polarization Curves of (1)  $\text{CuCl}_2$ , (2)  $\text{NiCl}_2$ , and (3)  $\text{FeCl}_2$

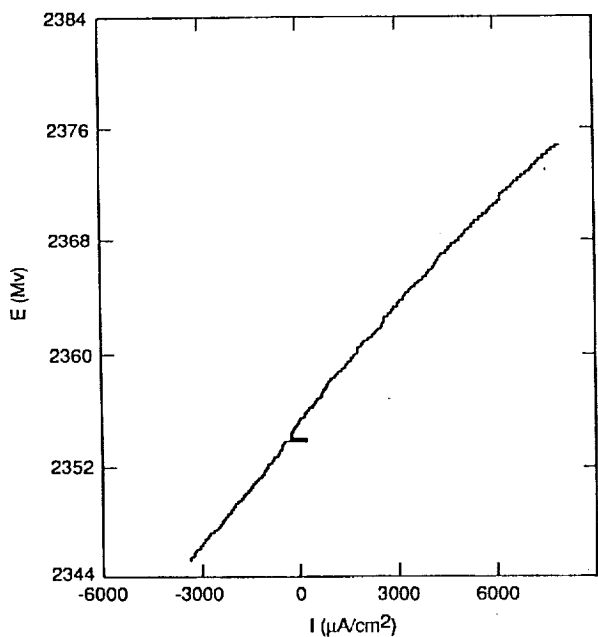


Figure 7. Linear Polarization Curve for  $\text{FeCl}_2$  from which an Exchange Current Density of  $1.5 \text{ mA/cm}^2$  is Calculated

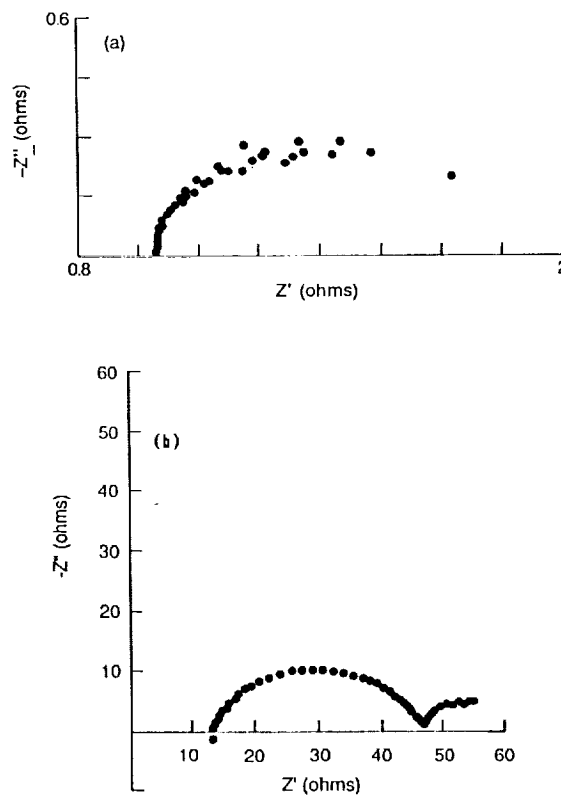


Figure 8. Complex Plane Impedance of (a)  $\text{NiCl}_2$  and (b)  $\text{CuCl}_2$

